# Supplementary Material for "TRACE: A Generalizable Drift Detector for Streaming Data-Driven Optimization"

**Yuan-Ting Zhong[1], Ting Huang[2], Xiaolin Xiao[3], Yue-Jiao Gong[1]***

[1]South China University of Technology
[2]Xidian University
[3]South China Normal University
{ytalienzhong, gnauhgnith, shellyxiaolin, gongyuejiao}@gmail.com

## A. Sequences Embedding Module of TRACE

In TRACE, input sequences vary in length due to the streaming nature of data. To ensure uniform input dimensions, sequences are padded to a predefined maximum length, with padding tokens assigned a value of positive infinity, which the model learns to ignore. The embedding and positional encoding modules transform the raw statistical feature sequences into structured, temporally aware representations, forming the basis for subsequent attention mechanisms.

We employ a multi-layer fully connected embedding block. This block enables the transformation of low-dimensional, hand-crafted statistical features into a semantically rich embedding space, thereby enhancing the model's capacity to distinguish intricate drift patterns. In addition, `Sin` positional encoding is added to the embedded vectors to retain the sequential order of the windows. Unlike fixed-length sequence models, this encoding is dynamically generated according to the actual sequence length, allowing for flexible input without loss of temporal information. The embedding procedure is formally defined as:

$$\begin{aligned} \mathbf{h}_i &= \text{LayerNorm}(\mathbf{W}_2 \cdot \phi(\mathbf{W}_1 \cdot \mathbf{fv}_i + \mathbf{b}_1) + \mathbf{b}_2) \\ \mathbf{H} &= [\mathbf{h}_0, \cdots, \mathbf{h}_T] \\ \mathbf{H}^{\text{pos}} &= \mathbf{H} + \mathbf{P} \end{aligned} \tag{1}$$

where $\mathbf{fv}_i \in \mathbb{R}^{d_f}$, is the input feature vector for the $i$-th window, $\phi(\cdot)$ is an activation function, $\mathbf{W}_1 \in \mathbb{R}^{d_1 \times d_f}$ and $\mathbf{W}_2 \in \mathbb{R}^{d_{\text{embed}} \times d_f}$ are learnable projection matrices, and $\mathbf{P} \in \mathbb{R}^{T \times d\text{embed}}$ denotes the positional encoding matrix.

## B. The Detection-Adaptation Loop of TRACE-EA

The pseudo code of TRACE-EA is provided in Algorithm 1.

## C. Detailed Experimental Setting

### C-1. Competitors: Concept drift detectors

- **DDM (Gama et al. 2004)** detects concept drift by monitoring the classifier's prediction error and its associated standard deviation over time. At each time step, the algorithm records the classification error and computes the running average error rate along with its standard deviation. Drift is signaled when the current error exceeds a statistically derived upper bound based on the historical minimum error rate plus a confidence margin. This approach effectively identifies significant degradation in predictive performance indicative of concept drift.
- **ADWIN (Bifet and Gavaldà 2007)** maintains an adaptive sliding window over the data stream, which is dynamically partitioned into two sub-windows. It continuously tracks the mean classification error, within each sub-window. Using Hoeffding's inequality, ADWIN performs a statistical hypothesis test to evaluate whether the difference between the means of these two sub-windows is statistically significant. If a significant difference is detected, which indicates a potential change in the data distribution. Consequently, it discards the older sub-window by truncating the window to exclude outdated data, thereby adapting to the new concept.
- **HDDM_A (Frias-Blanco et al. 2015)** maintains an optimal split point within the data stream that divides the recent data into two segments. Using a statistical hypothesis test grounded in Hoeffding's inequality, HDDM_A evaluates whether the difference between the distributions of data before and after this split point is statistically significant. A significant difference indicates the occurrence of concept drift, enabling timely detection of changes in the underlying data distribution.
- **HDDM_W (Frias-Blanco et al. 2015)** maintains an optimal split point within the data stream and computes the current classifier's prediction error using an exponential weighting scheme to emphasize recent instances. Employing a statistical hypothesis test based on McDiarmid's inequality, HDDM_W assesses whether there is a significant difference between the data distributions before and after the split point. Detection of a statistically significant difference signals the occurrence of concept drift, allowing for timely adaptation to changes in the data stream.
- **FHDDM (Pesaranghader and Viktor 2016)** employs a sliding window to monitor the proportion of correctly classified samples within the current window. It compares this accuracy against the maximum historical accuracy observed, using Hoeffding's inequality to establish a

*Corresponding author

Algorithm 1: TRACE-EA

**Input**: $\{\cdots, \mathbb{D}_t, \cdots\}$: Streaming data; $\mathrm{arc}_{\max}$: Maximum archive size; $T$: Token sequence length parameter (the maximum sequence length is $T+1$);
TRACE: Drift detector.
**Output**: Optimal solution for time $t$.

$Arc \leftarrow \varnothing$, $k \leftarrow 1$, $WS \leftarrow \varnothing$
$m_k$, $P_k^{\mathrm{opt}} \leftarrow$ InitializeEnv($\mathbb{D}_{\text{init}}$)
$Arc \leftarrow Arc \cup \{\{\mathbb{D}_{\text{init}}, m_k, P_k^{\mathrm{opt}}\}\}$
**while** not the end of data stream **do**
  $WS \leftarrow WS \cup \mathbb{D}_t$
  $\mathbb{D}_k, m_k, P_k^{\mathrm{opt}} \leftarrow Arc(k)$
  $TS \leftarrow$ GetWindowSeq($WS$,$\mathbb{D}_k$)
  $dl \leftarrow$ TRACE($TS$)
  **if** $dl \in [1, \cdots, T]$ **then**
    $k \leftarrow k+1$
    $\mathbb{D}_{\text{new}} \leftarrow WS(dl+1:)$
    $m_k$, $P_k^{\mathrm{opt}} \leftarrow$ NewEnv($Arc$, $\mathbb{D}_{\text{new}}$)
    $n \leftarrow |\mathbb{D}_k| + |\mathbb{D}_t|$
  **else if** n mod $u$ = 0 **then**
    $m_k \leftarrow$ UpdateModel($\mathbb{D}_k$)
  **end if**
  $P_k \leftarrow$ ReusePopulation($Arc$)
  $M_k \leftarrow$ AssignWeight($Arc$)
  $P_k^{\mathrm{opt}} \leftarrow$ EvolvePopulation($P_k$, $M_k$)
  $\mathbb{D}_k \leftarrow \mathbb{D}_k \cup \mathbb{D}_t$
  $Arc \leftarrow Arc \cup \{\{\mathbb{D}_k, m_k, P_k^{\mathrm{opt}}\}\}$
  $WS \leftarrow WS(dl+1:)$
  **if** len($Arc$) $> \mathrm{arc}_{\max}$ **then**
    $Arc \leftarrow Arc$ / $\{Arc(1)\}$
    $k \leftarrow k-1$
  **end if**
  **return** $P_k^{\mathrm{opt}}(1)$
**end while**

statistical threshold. When the current accuracy falls significantly below this threshold, the method signals that concept drift has occurred.

- **KSWIN (Raab, Heusinger, and Schleif 2020)** maintains a fixed-size sliding window over the data stream, which is split into two sub-windows: a recent window and a reference window. The algorithm applies the Kolmogorov-Smirnov statistical test to compare the distributions of data in these two sub-windows. If the test detects a significant difference exceeding a predefined threshold, concept drift is detected.
- **RADAR (Alsaedi et al. 2023)** is an unsupervised concept drift detection method that utilizes two sliding windows and cyclic variational inference (RVE) to embed data samples into a high-dimensional latent space. It computes a change score based on the distance relationships among samples within this latent space. Using a statistical test analogous to Gaussian error boundary assessment, RADAR detects drift when the change score exceeds a predefined threshold, signaling a significant shift in the data distribution.
- **MCD-DD (Wan, Liang, and Yoon 2024)** employs a deep contrastive learning framework based on the maximum concept discrepancy (MCD) principle. It constructs two sliding windows to sample positive and negative pairs, optimizing a contrastive loss that pulls positive pairs closer and pushes negative pairs apart in the latent space. Concept drift is detected when the distance between contrastive samples pair surpasses a dynamically adjusted threshold, indicating significant changes in the underlying data distribution.
- **HCDD (Zhong and Gong 2025)** applies three level confidence strategy for the drift detection. It operates on a moving window to handle continuously streaming data. It monitors model's error-rate deviations for incoming data using multiple confidence levels of warning intervals. This hierarchical approach enables more precise and adaptive detection of various types of concept drifts.

To adapt the evaluated methods to regression-type optimization problems, we made minimal modifications while preserving the core logic of each detector. Specifically, for DDM, ADWIN, KSWIN, RADAR and MCD-DD, we directly replaced the original classifier-based error with the error rate $er$. For ADWIN, this error rate was truncated to the range $[0, 1]$ to satisfy its statistical assumptions by Hoeffding's inequality. For methods originally designed for binary feedback, HDDM_A, HDDM_W and FHDDM, we applied a binarization process: the continuous error rate was thresholded at 0.3, where values above the threshold were mapped to 0 (indicating wrong classification), and values below or equal to the threshold were mapped to 1 (indicating correct classification). The experimental setup is as follows: a total of 600 environments were generated, the number of instances in each environment is randomly selected from the set $\{100, 200, 300\}$. The drift detection tolerance was set equal to the environment size; that is, if a detection method identifies a drift within the corresponding environment, it is considered a true positive. All other parameters were kept consistent with the original settings reported in the respective original papers.

## C-2. Competitors: SDDEAs

- **SAEF-1GP (Luo et al. 2019)** adopts a memory-based strategy that preserves high-quality solutions obtained from recent environments. These stored solutions are integrated into the dataset used to construct surrogate models for the new environment, enhancing model accuracy and generalization. Additionally, the retained solutions are used to replace inferior individuals in the initial population, thus promoting a more efficient search for optimal solutions. The 1GP version, which utilizes GP as surrogate models with a single population, is selected for comparison due to its notable performance.
- **BDDEA-LDG (Li et al. 2020)** adopts a perturbation-based strategy to generate synthetic data samples within the current environment, assigning pseudo-labels to these samples based on their nearest labeled neighbors. A

boosting framework is then applied to train an ensemble of base models using the augmented dataset. This approach not only increases the volume of training data but also enhances model diversity, thereby improving overall predictive performance and robustness in dynamic environments.

- **TT-DDEA (Huang, Wang, and Jin 2021)** leverages a tri-training strategy to construct surrogate models tailored to the current environment. Throughout the evolutionary process, newly generated individuals are treated as unlabeled data. In each iteration, three individuals with the most confident predictions are identified and used to incrementally fine-tune the surrogate models. This iterative self-labeling mechanism progressively enhances model accuracy and supports more effective optimization.
- **DSEMFS (Yang et al. 2023)** employs a model pool in which each surrogate model is assigned a weight based on its root mean squared error (RMSE) evaluated on the current environment. These weighted models are then aggregated to form an ensemble surrogate model tailored for the new environment. The ensemble model guides a multi-task evolutionary algorithm in solving the optimization problem within the current environment.
- **DETO (Li, Chen, and Yao 2024)** employs clustering techniques to group Multi-Output Gaussian Process model parameters collected from past environments. It identifies clusters and selects optimal solutions from environments nearest to the cluster centroids to augment the current dataset. This enriched data supports the construction of a more informative surrogate model. Finally, a DE algorithm enhanced with local search strategies is applied to efficiently explore and optimize the problem in the new environment.
- **MLDE (Zhang et al. 2024)** proposes a meta-learning framework that leverages surrogate model transfer across environments. Specifically, it stores the surrogate model parameters from randomly selected environments and, upon entering a new environment, evaluates these models based on their mean squared error (MSE) on the current environment's data. The model with the lowest MSE is selected, and its parameters are used to initialize the surrogate model for the new environment. This surrogate model is then employed to guide the optimization process. We choose the DE algorithm as the optimizer for its excellent performance.
- **DASE (Zhong and Gong 2025)** is the first drift-aware approach proposed for SDDO. It employs a hierarchical confidence-based drift detector to identify distributional shifts in the environment. Upon detecting a drift, DASE activates a context-aware warm-start mechanism that adaptively transfers knowledge from historical environments, using a similarity-based weighting strategy to prioritize knowledge from relevant past environments.

In the experiments, all methods are provided with an equal number of data points to ensure a fair comparison. It is important to note that our proposed algorithm operates in a passive data acquisition setting, whereas MLDE, DETO, and SAEF-1GP adopt active-query strategies, where new data points are selectively queried during the optimization process. To adapt these active-query based SDDEAs to passive-query framework, modifications are made accordingly. For MLDE, both the support and query sets are drawn directly from the existing data stream without acquiring new samples. Specifically, for each environment, $2k$ data points are stored, with $k$ points serving as the support set and the other $k$ points as the query set, and $k$ is set to 5 following the original paper (Zhang et al. 2024). For DETO, real fitness evaluations of the best-found solutions are replaced with predictions from the surrogate models to avoid new queries. For SAEF-1GP, the surrogate model is updated only once at the start of the optimization process, and subsequent updates during optimization iterations are omitted, in line with the setting used in (Yang et al. 2023).

## C-3. Benchmarks

The benchmark instances utilized in our experiments are summarized in Table 1 (DBG), Table 2 (GMPB), and Table 3 (SDDObench).

- **DBG (Li et al. 2008)** introduces a generalized dynamic benchmark generator specifically tailored for dynamic optimization problems. It includes two classes of objective functions. The first class consists of a dynamic rotation peak generator (F1). The second category (F2 to F6) contains dynamic composition functions constructed from a combination of basic functions including sphere, Rastrigin, Weierstrass, Griewank and Ackley. These functions are composed using dynamic weighting strategies and spatial transformations. DBG provides six types of dynamic changes, including small step changes, large step changes, random changes, chaotic changes, recurrent changes, and recurrent changes with noise.
- **GMPB (Yazdani et al. 2022)** presents a benchmark suite based on generalized moving peak functions, which is designed to emulate complex, high-dimensional, and non-separable dynamic environments. GMPB supports various landscape features, such as a configurable number of sub-functions, different conditioning levels, component separability, modality. These features are controlled through flexible parameter configurations, allowing researchers to systematically analyze algorithm performance across a broad range of challenges. The benchmark includes eight representative instances (F1 to F8), each reflecting distinct characteristics in terms of modality, severity of change, and dimensionality.
- **SDDObench (Zhong et al. 2024)** comprises eight benchmark functions designed to evaluate streaming data-driven optimization methods. The first three instances (F1 to F3) are based on Multi-Peak Functions (MPFs), constructed to assess the algorithm's ability to handle dynamic changes in peak location, height, and width. The remaining five instances (F4 to F8) are adapted from common used objective functions for DDEAs (DCF). To simulate realistic streaming environments, SDDObench also provides five types of concept drift: no drift, sudden drift, recurrent sudden drift, re-

current incremental drift, and recurrent incremental drift with noise, to create a more dynamic and challenging optimization landscape.

### C-4. Training setting of TRACE

We utilize *SDDObench* (Zhong et al. 2024), employing a distinct set of problem instances generated with configurations explicitly disjoint from those used during training. Specifically, training set uses more severe shifts with parameters $\mathcal{I}_h = 0.4$, $\mathcal{I}_w = 0.3$, and $\mathcal{I}_x = 0.5$, while evaluation adopts milder settings $\mathcal{I}_h = 0.3$, $\mathcal{I}_w = 0.1$, and $\mathcal{I}_x = 0.4$ to simulate moderate and realistic drifts. This setup enables a rigorous assessment of TRACE's generalization within the same distribution.

### C-5. Performance Metrics

The primary metric used to evaluate drift detectors is *Precision* and *F1*, defined as:

$$\begin{aligned} Precision &= \frac{TP}{TP + FP} \\ Recall &= \frac{TP}{TP + FN} \\ F1 &= 2 \cdot \frac{Precision \cdot Recall}{Precision + Recall} \end{aligned} \tag{2}$$

where $TP$ denotes the number of true positives (correctly detected drift points), $FP$ the false positives (incorrect drift alarms), and $FN$ the false negatives (missed true drift points).

Precision and F1 are chosen as the key metric because they directly measure the reliability of drift detection —the probability that a detected drift corresponds to an truly concept drift. In continuously streaming optimization environments, false positives may lead to unnecessary model resets or updates, potentially disrupting the optimization process. Therefore, maintaining high precision is critical for ensuring algorithmic stability and efficiency.

For evaluating SDDEAs, we use the widely adopted *Dynamic Tracking Error*, which quantifies the average discrepancy between the best-found solution and the true global optimum over time. Formally, it is expressed as:

$$E_{\mathrm{DT}} = \frac{1}{N_t I} \sum_{t=1}^{N_t} \sum_{i=1}^{I} \left[ f(x^{*((t-1)I+i)}) - f(x^{\star(t)}) \right] \tag{3}$$

where $N_t$ is the total number of time points, $I$ number of iterations per time point; $x^{*((t-1)I+i)}$ is the best solution found at the $i$-th iterative evaluation in the $t$-th time point, $x^{\star(t)}$ is the global optimum at time $t$.

The $E_{\mathrm{DT}}$ metric provides an aggregate measure of algorithm performance across dynamic environments.

## D. Detailed Experimental results

This section presents comprehensive experimental results comparing the proposed TRACE framework with existing methods. The performance is evaluated on both in-distribution and out-of-distribution scenarios using three benchmark suites: SDDObench, DBG, and GMPB.

### D-1. Detailed Experiments of Detector Performance Comparison

The complete comparison results are provided in the Figure 1.

### D-2. Detailed Experiments of SDDO Performance Comparison

This part is the detailed experimental results of SDDO performance comparison.

*1) Performance of In-Distribution (ID) benchmark:* As shown in Table 4, TRACE consistently outperforms all baseline algorithms across all benchmark instances within the SDDObench suite. This result demonstrates the strong effectiveness of TRACE in handling ID problems, where the training and testing environments share similar statistical properties. Notably, TRACE achieves superior performance in both MPF (F1-F3) and DCF (F4-F8), indicating its ability to adapt to different types of landscape dynamics such as shifting peak locations, heights, and widths. The improvement over other SDDEAs, such as DETO, MLDE, and DSEMFS, suggests that TRACE benefits from its transferable pattern-learning capability and its ability to capture temporal dependencies in the data stream.

*2) Performance of Out-Of-Distribution (OOD) Benchmarks:* Tables 5 and 6 provide the performance comparison of TRACE-EA with baseline methods on the DBG and GMPB benchmarks, which represent OOD scenarios. These results highlight the generalization capability of TRACE when evaluated on problem settings that differ significantly from those seen during training.

On the DBG benchmark (Tables 5), TRACE-EA exhibits robust performance across both rotation-based and composition-based dynamic functions. Despite the diversity in landscape characteristics and the inclusion of various types of dynamic changes (e.g., chaotic, random, recurrent with noise), TRACE-EA maintains competitive or superior accuracy. This indicates that the learned drift patterns in TRACE are not overly fitted to the specific structure of SDDObench and can transfer effectively to unseen dynamic drift patterns.

Similarly, on the GMPB benchmark (Tables 6), TRACE-EA demonstrates high adaptability across a wide range of dynamic landscapes with different sub-function structures, conditioning levels, and variable interaction patterns. Even in challenging scenarios with high ill-conditioning or non-separable variables (F5, F7, F8), TRACE-EA consistently ranks among the top performers. This confirms that TRACE is not only effective in capturing recurrent temporal regularities but also capable of generalizing to previously unseen distribution shifts and optimization structures.

In summary, the experimental results across all benchmarks show that TRACE and TRACE-EA achieve both strong ID performance and promising OOD generalization. This underscores the effectiveness of the proposed dual-attention architecture in learning transferable drift patterns and adapting to a wide variety of dynamic optimization environments.

Table 1: The problem instances and parameter configuration of DBG

| | | |
|---|---|---|
| **Problem Definition** | $F = f(x, \phi, t)$<br>$\phi(t+1) = \phi(t) \oplus \Delta\phi$ | |
| **Problem Instance** | F1: Rotation peak function<br>$f(x,\phi,t) = \min_{i=1}^{m} \left\{ \vec{H}_i(t) / \left(1 + \vec{W}_i(t) \cdot \sqrt{\sum_{j=1}^{d} \frac{(x_j - \vec{X}_j^i(t))^2}{d}}\right)\right\}$<br>$\vec{H}_i(t)$: The height of the $i$-th peak in the $t$-th time point.<br>$\vec{W}_i(t)$: The width of the $i$-th peak in the $t$-th time point.<br>$\vec{X}^i(t)$: The central position of the $i$-th peak in the $t$-th time point. | |
| | F2-F6: Composition function<br>$F(x,\phi,t) = \sum_{i=1}^{n}(w_i \cdot (f_i((x - \vec{O}_i(t) + O_{iold})/\lambda_i \cdot \vec{M}_i) + \vec{H}_i(t)))$<br>$w_i$: the weight of the $i$-th baseline function.<br>$\vec{O}_i(t)$: The optimal value of the basis function changed by rotation at time $t$;<br>$O_{iold}$; The optimal value of the base function before the change<br>(this value is 0 for the following five functions);<br>$\lambda_i$: The scaling coefficient of the $i$th basis function;<br>$\vec{M}_i$: The orthogonal rotation matrix corresponding to the $i$th basis function; | |
| | F2: Composition of Sphere's function<br>F3: Composition of Rastrigin's function<br>F4: Composition of Griewank's function<br>F5: Composition of Ackley's function<br>F6: Hybrid Composition function | |
| **Baseline function** | Equation | Variables Range |
| Sphere | $\sum_{i=1}^{d} x_i^2$ | $[-100, 100]$ |
| Rastrigin | $\sum_{i=1}^{d}(x_i^2 - 10cos(2\pi x_i) + 10)$ | $[-5, 5]$ |
| Weierstrass | $\sum_{i=1}^{d}\left(\sum_{k=0}^{k_{\max}}\left(a^k cos(2\pi b^k(x_i + 0.5))\right)\right) - d\sum_{k=0}^{k_{\max}}\left(a^k cos(\pi b^k)\right)$<br>$a = 0.5, b = 3, k_{\max} = 20$ | $[-0.5, 0.5]$ |
| Griewank | $\frac{1}{4000}\sum_{i=1}^{d} x_i^2 - \prod_{i=1}^{d} cos(\frac{x_i}{\sqrt{i}}) + 1$ | $[-100, 100]$ |
| Ackley | $-20\exp\left(-0.2\sqrt{\frac{1}{d}\sum_{i=1}^{d} x_i^2}\right) - \exp\left(\frac{1}{n}\sum_{i=1}^{d} cos(2\pi x_i)\right) + 20 + e$ | $[-32, 32]$ |
| **Dynamic Change** | C1: small step change<br>$\Delta\phi = \alpha \cdot \|\|\phi\|\| \cdot r \cdot \phi_{severity}$ | |
| | C2: large step change<br>$\Delta\phi = \|\|\phi\|\| \cdot (\alpha \cdot sign(r) + (\alpha_{max} - \alpha) \cdot r) \cdot \phi_{severity}$ | |
| | C3: random change<br>$\Delta\phi = N(0,1) \cdot \phi_{severity}$ | |
| | C4: chaotic change<br>$\phi(t+1) = A \cdot (\phi(t) - \phi_{min}) \cdot (1 - (\phi(t) - \phi_{min})/\|\|\phi\|\|)$ | |
| | C5: recurrent change<br>$\phi(t+1) = \phi_{min} + \|\|\phi\|\|(sin(\frac{2\pi}{P}t + \varphi) + 1)/2$ | |
| | C6: recurrent change with noise<br>$\phi(t+1) = \phi_{min} + \|\|\phi\|\|(sin(\frac{2\pi}{P}t + \varphi) + 1)/2 + N(0,1) \cdot noisy_{severity}$ | |
| | C7: dimension change<br>$d(t+1) = d(t) + sign \cdot \Delta d$ | |
| | $\|\|\phi\|\|$: Range of $\phi$;<br>$\phi_{severity}$: Constant —indicates the degree of change in the variable;<br>$noisy_{severity}$: The intensity of noise;<br>$\alpha \in (0,1)$, $\alpha_{max} \in (0,1)$: Set to 0.04 and 0.1 respectively;<br>$A \in (1,4)$: A positive constant $r \in (-1,1)$: A random value;<br>$sign(x) = 1$, if $x > 0$; otherwise $sign(x) = 0$;<br>$N(0,1)$: Represents a random number sampled from a standard normal distribution.<br>$\Delta d$: The default setting is 1;<br>When the dimension is reduced, remove from the last dimension of the variable. | |

Table 2: The problem instances and parameter configuration of GMPB

| **Problem Definition** | $F^{(t)}(\mathbf{x}) = d^{-1}\sum_{i=1}^{k} d_i f_i^{(t)}(\mathbf{x})$ |
|---|---|
| **Components** | |
| Moving Peak Function $f^{(t)}(\mathbf{x})$ | $f^{(t)} = \min\limits_{i\in\{1,\dots,m\}} \left\{ h_i^{(t)} - \sqrt{\mathbb{T}\left(\left(\mathbf{x}-\mathbf{c}_i^{(t)}\right)^{\top}\mathbf{R}^{(t)\top}, i\right)\mathbf{W}^{(t)}\mathbb{T}\left(\mathbf{R}^{(t)}\left(\mathbf{x}-\mathbf{c}_i^{(t)}\right), i\right)} \right\}$<br>$h_i^{(t)}, \mathbf{c}_i^{(t)}$: the height and central position for $i$-th peak respectively;<br>$\mathbf{W}^{(t)} = (w_i^{(t)})^2\mathbf{I}$: the width for $i$-th peak. |
| Rotation Matrix $\mathbf{R}^{(t)}$ | $\mathbf{R}_i^{(t)} = \prod\limits_{(p,q)\in\mathcal{P}} \mathbf{G}_{(p,q)} \times \mathbf{R}_i^{(t-1)}$<br>$\mathbf{G}_{(p,q)}(p,p) = \cos\left(\theta^{(t)}\right)$<br>$\mathbf{G}_{(p,q)}(q,q) = \cos\left(\theta^{(t)}\right)$<br>$\mathbf{G}_{(p,q)}(p,q) = -\sin\left(\theta^{(t)}\right)$<br>$\mathbf{G}_{(p,q)}(q,p) = \sin\left(\theta^{(t)}\right)$ |
| Asymmetric Transform Matrix $\mathbb{T}(\mathbf{y}, i)$ | $\mathbb{T}(y_j, i) = \begin{cases} \exp\left(\log(y_j) + \tau_i^{(t)}\left(\sin\left(\eta_{i,1}^{(t)}\log(y_j)\right) + \sin\left(\eta_{i,2}^{(t)}\log(y_j)\right)\right)\right) & \text{if } y_j > 0 \\ 0 & \text{if } y_j = 0 \\ -\exp\left(\log(\lvert y_j\rvert) + \tau_i^{(t)}\left(\sin\left(\eta_{i,3}^{(t)}\log(\lvert y_j\rvert)\right) + \sin\left(\eta_{i,4}^{(t)}\log(\lvert y_j\rvert)\right)\right)\right) & \text{if } y_j < 0 \end{cases}$<br>$\tau_i^{(t)}$,$\eta_{i,k}^{(t)}, k = 1\cdots,4$: control irregularities and problem characteristics. |
| **Dynamic Change** | $\mathbf{c}_{i,j}^{(t+1)} = \mathbf{c}_{i,j}^{(t)} + \tilde{s}_i \frac{\mathbf{r}}{\lVert\mathbf{r}\rVert}$<br>$h_{i,j}^{(t+1)} = h_{i,j}^{(t)} + \tilde{h}_i\mathcal{N}(0,1)$<br>$w_{i,j,k}^{(t+1)} = w_{i,j,k}^{(t)} + \tilde{w}_i\mathcal{N}(0,1)$<br>$\theta_{i,j}^{(t+1)} = \theta_{i,j}^{(t)} + \tilde{\theta}_i\mathcal{N}(0,1)$<br>$\eta_{i,j,l}^{(t+1)} = \eta_{i,j,l}^{(t)} + \tilde{\eta}_i\mathcal{N}(0,1), l \in \{1,2,3,4\}$<br>$\tau_{i,j}^{(t+1)} = \tau_{i,j}^{(t)} + \tilde{\tau}_i\mathcal{N}(0,1)$<br>$\mathcal{N}(0,1)$: a random number sampled from a standard normal distribution;<br>$\tilde{h}_i$: height of the $i$-th sub-function;<br>$\tilde{w}_i$: width of the $i$-th sub-function;<br>$\tilde{s}_i$: shift value of the $i$-th sub-function;<br>$\tilde{\theta}_i$: angle of the $i$-th sub-function;<br>$\tilde{\eta}_i$, $\tilde{\tau}_i$: change parameter for asymmetric transformation of the $i$-th sub-function;<br>$w_{i,j,k}$: the width of the $j$-th peak in the $k$-th dimension of the $i$th sub-function. |

Table 3: The problem instances and parameter configuration of SDDObench

| **Ins.** | **Objective Function** | **Transformation Function** | **Variables Range ($\phi$)** | **Optimum** | **Parameters Setting** |
|---|---|---|---|---|---|
| F1 | $f_{MPF}$ | $x^{(t)} = x^{(t_0)}$<br>for $peak_i$,<br>$h_i^{(t)} = g(h_i^{(t_0)}, \delta(t))$<br>$w_i^{(t)} = g(w_i^{(t_0)}, \delta(t))$<br>$c_i^{(t)} = g(c_i^{(t_0)}, \delta(t))$ | $h \in [-70, -30]$<br>$w \in [1, 12]$<br>$c \in [-5, 5]^d$<br>$x \in [-5, 5]^d$<br>$m^{(t_0)} = 8$ | $\min\limits_{j}^{m} h_j$ | intensities: $\mathcal{I}_h = 0.3$,<br>$\mathcal{I}_w = 0.1, \mathcal{I}_c = 0.4$,<br>$\mathcal{I}_x = 0.4, \mathcal{I}_m = 0.5$<br>offset: $\epsilon = 0.3$<br>sudden number: $\lvert\Lambda\rvert = 5$<br>change rate: $r_c = 0.5$<br>recurrent period: $P = 20$ |
| F2 | $f_{MPF}$ | randomly select $\lceil r_c \cdot m \rceil$ peaks,<br>if $peak_i$ is selected, as F1,<br>otherwise,<br>$h_i^{(t)} = h_i^{(t-1)}$<br>$w_i^{(t)} = w_i^{(t-1)}$<br>$c_i^{(t)} = c_i^{(t-1)}$ | as F1 | | |
| F3 | $f_{MPF}$ | as F1, and<br>$m^{(t)} = g(m^{(t_0)}, \delta(t))$ | as F1, and<br>$m \in [3, 40]$ | | |
| F4 | $f_{DCF}$ : Sphere | $x^{(t)} = g(x^{(t_0)}, \delta(t))$ | $x \in [-5.12, 5.12]^d$ | 0 | |
| F5 | $f_{DCF}$ : Rosenbrock | as F4 | $x \in [-2.048, 2.048]^d$ | | |
| F6 | $f_{DCF}$ : Ackley | as F4 | $x \in [-32.768, 32.768]^d$ | | |
| F7 | $f_{DCF}$ : Griewank | as F4 | $x \in [-600, 600]^d$ | | |
| F8 | $f_{DCF}$ : Rastrigin | as F4 | $x \in [-5.12, 5.12]^d$ | | |

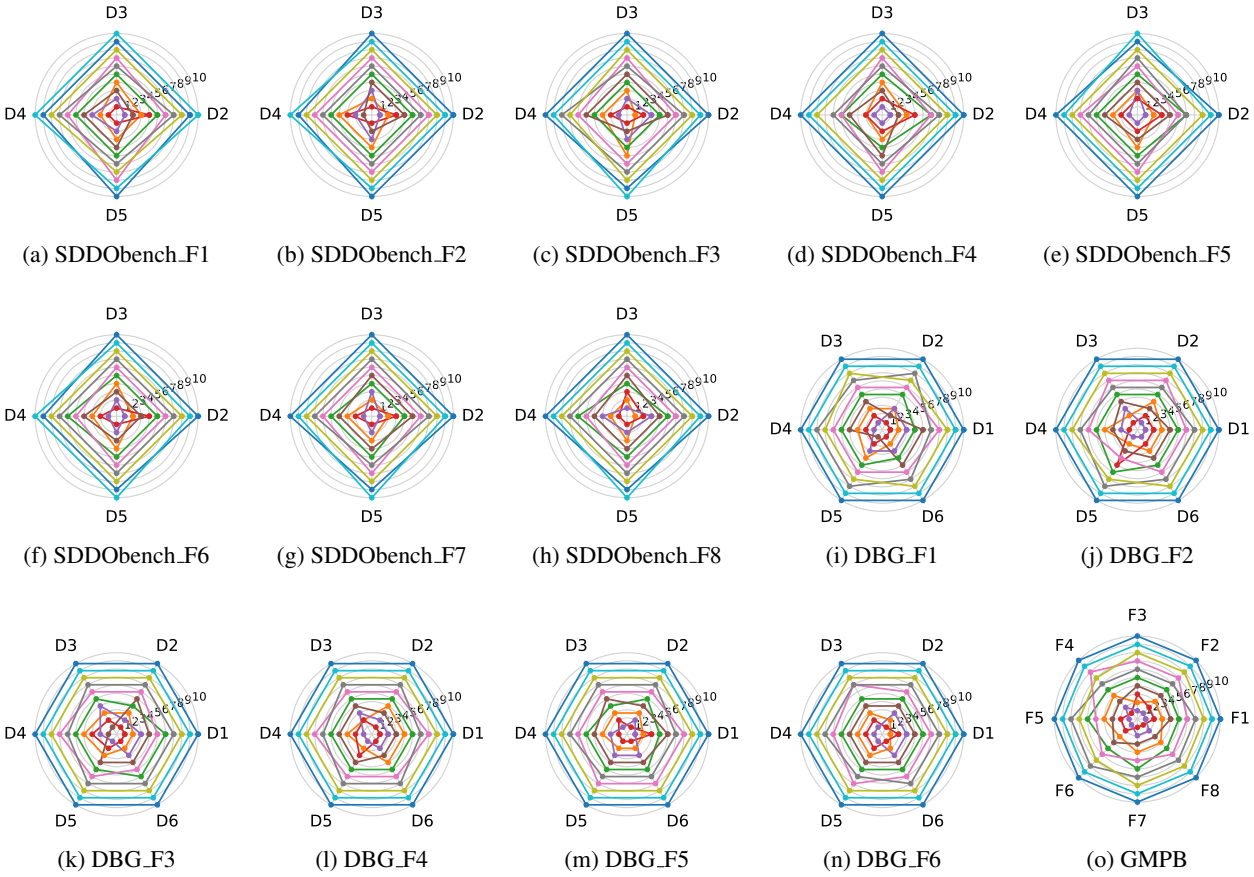


(a) SDDObench_F1 (b) SDDObench_F2 (c) SDDObench_F3 (d) SDDObench_F4 (e) SDDObench_F5

(f) SDDObench_F6 (g) SDDObench_F7 (h) SDDObench_F8 (i) DBG_F1 (j) DBG_F2

(k) DBG_F3 (l) DBG_F4 (m) DBG_F5 (n) DBG_F6 (o) GMPB

Figure 1: Precision comparison of TRACE and compared methods across different drift types and benchmarks.

### D-3. Plug-and-Play capability of TRACE

Table 7 presents the evaluation results of integrating TRACE into four representative dynamic optimization frameworks: DASE, MLDE, DETO, and TT-DDEA. These experiments are conducted on the SDDObench suite to assess the plug-and-play capability of TRACE (its ability to enhance existing algorithms).

The results clearly demonstrate that incorporating TRACE leads to substantial performance improvements across all tested algorithms. This highlights the compatibility and flexibility of TRACE as a general-purpose drift detection module that can be seamlessly embedded into any SDDEAs. Notably, the performance gains are especially significant in more complex problem instances, such as F7 and F8. These instances are characterized by intricate landscape changes involving varying modalities and complex drift patterns. In such scenarios, TRACE provides more accurate and timely drift detection, which enables the optimization process to adjust its search behavior more responsively. As a result, the algorithms equipped with TRACE exhibit better adaptability and convergence efficiency in streaming environments. Overall, these findings highlight the practicality of TRACE as a drift-aware modular enhancement component for SDDEAs.

### D-4. Detection Delay and Computation Cost Comparison Results

As shown in Table 8, TRACE significantly reduces detection delay across all tested drift types, demonstrating its ability to identify complex patterns earlier than statistical methods. We also assessed mean inference time and peak memory usage among the above methods in Table 9. While more resource-intensive than simple methods like DDM, HCDD, TRACE achieves an inference speed comparable to ADWIN, being $\sim 40\times$ faster and using $\sim 4.5\times$ less memory than powerful competitors like RADAR. This strikes an excellent balance between performance and practical deployment cost.

## E. Real-World Datasets for Streaming Cluster

To evaluate the practical applicability of the proposed method in realistic non-stationary environments, we employ four widely-used real-world datasets for stream clustering tasks. These datasets are characterized by high volume, temporal evolution, and varying distributional patterns, making them well-suited for assessing the robustness and adaptability of clustering algorithms under concept drift. Stream clustering is a fundamental task in data stream mining (Chen and Shang 2019), where the goal is to assign observations to

Table 4: Comparison of the mean and standard deviation over 11 independent runs of $E_{\mathrm{DT}}$ values achieved by different SDDEAs on the SDDObench benchmark with 10-dimensional decision variables.

| Instance | Drift | TRACE-EA | SAEF-1GP | BDDEA-LDG | TT-DDEA | DSEMFS | DETO | MLDE | DASE |
|---|---|---|---|---|---|---|---|---|---|
| F1 | D1 | **6.52e+01±1.52e-02** | 6.80e+01±3.43e+00 (+) | 6.81e+01±1.76e+00 (+) | 6.80e+01±2.10e+00 (+) | 6.78e+01±5.57e-01 (+) | 6.81e+01±6.16e-01 (+) | 6.81e+01±3.65e-02 (+) | 6.55e+01±2.23e-02 (≈) |
| | D2 | **6.53e+01±4.90e-01** | 6.57e+01±1.78e+00 (+) | 6.66e+01±4.10e+00 (+) | 6.68e+01±2.46e+00 (+) | 6.73e+01±2.90e-02 (+) | 6.70e+01±1.01e+00 (+) | 6.70e+01±3.33e-02 (+) | 6.61e+01±1.33e-01 (+) |
| | D3 | **6.37e+01±1.42e-01** | 6.58e+01±6.11e+00 (+) | 6.55e+01±3.37e+00 (+) | 6.57e+01±1.40e+00 (+) | 6.56e+01±1.52e-02 (+) | 6.59e+01±1.55e+00 (+) | 6.59e+01±1.95e-02 (+) | 6.40e+01±2.51e-01 (+) |
| | D4 | **6.40e+01±1.77e-01** | 6.50e+01±1.92e+00 (+) | 6.48e+01±1.13e-02 (+) | 6.49e+01±2.07e+00 (+) | 6.50e+01±2.97e+00 (+) | 6.51e+01±2.36e+00 (+) | 6.51e+01±5.06e-02 (+) | 6.39e+01±1.33e-01 (≈) |
| | D5 | **6.41e+01±1.73e-01** | 6.51e+01±3.97e+00 (+) | 6.49e+01±1.18e-02 (+) | 6.51e+01±2.28e-02 (+) | 6.52e+01±2.87e-02 (+) | 6.53e+01±2.69e+00 (+) | 6.52e+01±3.92e-02 (+) | 6.45e+01±1.04e-01 (≈) |
| F2 | D1 | **6.69e+01±6.51e-01** | 6.80e+01±2.27e+00 (+) | 6.81e+01±1.42e-02 (+) | 6.80e+01±4.20e+00 (+) | 6.78e+01±1.92e-02 (+) | 6.81e+01±1.30e+00 (+) | 6.81e+01±7.82e-02 (+) | 6.76e+01±2.64e-01 (+) |
| | D2 | **6.52e+01±4.50e-01** | 6.57e+01±2.93e-02 (+) | 6.75e+01±2.55e-01 (+) | 6.74e+01±5.60e-01 (+) | 6.41e+01±4.42e-01 (+) | 6.73e+01±4.86e-01 (+) | 6.72e+01±5.40e-01 (+) | 6.68e+01±1.56e-01 (+) |
| | D3 | **6.50e+01±3.33e-01** | 6.60e+01±1.04e-02 (+) | 6.75e+01±3.93e-01 (+) | 6.70e+01±6.14e-01 (+) | 6.68e+01±4.67e-01 (+) | 6.72e+01±4.15e-01 (+) | 6.75e+01±4.17e-01 (+) | 6.54e+01±4.10e-01 (≈) |
| | D4 | **6.40e+01±6.93e-01** | 6.50e+01±2.34e+00 (+) | 6.82e+01±5.33e-01 (+) | 6.72e+01±7.06e-01 (+) | 6.70e+01±9.65e-01 (+) | 6.67e+01±6.87e-01 (+) | 6.70e+01±8.26e-01 (+) | 6.43e+01±7.32e-01 (≈) |
| | D5 | **6.44e+01±7.12e-01** | 6.53e+01±4.54e+00 (+) | 6.76e+01±4.44e-01 (+) | 6.75e+01±9.29e-01 (+) | 6.72e+01±5.42e-01 (+) | 6.64e+01±1.66e+00 (+) | 6.73e+01±9.46e-01 (+) | 6.52e+01±1.02e-02 (+) |
| F3 | D1 | **6.70e+01±1.03e-01** | 6.80e+01±5.56e-01 (+) | 6.81e+01±2.21e+00 (+) | 6.80e+01±3.91e+00 (+) | 6.78e+01±2.26e-02 (+) | 6.81e+01±3.43e+00 (+) | 6.81e+01±1.90e-02 (+) | 6.77e+01±1.26e-02 (+) |
| | D2 | **6.50e+01±1.14e-01** | 6.51e+01±1.47e+00 (+) | 6.65e+01±1.35e-02 (+) | 6.64e+01±2.72e-02 (+) | 6.67e+01±2.01e-02 (+) | 6.66e+01±4.83e-02 (+) | 6.65e+01±4.12e-02 (+) | 6.58e+01±7.68e-02 (+) |
| | D3 | **6.20e+01±2.28e-01** | 6.29e+01±7.54e-01 (+) | 6.34e+01±4.73e-02 (+) | 6.34e+01±6.65e-02 (+) | 6.37e+01±8.39e-02 (+) | 6.34e+01±3.38e+00 (+) | 6.34e+01±4.80e-02 (+) | 6.23e+01±4.11e-02 (≈) |
| | D4 | **6.23e+01±1.12e-02** | 6.30e+01±1.79e-02 (+) | 6.31e+01±7.79e-02 (+) | 6.30e+01±8.35e-02 (+) | 6.34e+01±1.15e-01 (+) | 6.32e+01±3.36e+00 (+) | 6.32e+01±8.46e-02 (+) | 6.25e+01±2.08e-02 (≈) |
| | D5 | **6.21e+01±1.69e-02** | 6.31e+01±7.32e-01 (+) | 6.32e+01±9.16e-02 (+) | 6.30e+01±1.44e-01 (+) | 6.34e+01±9.41e-02 (+) | 6.34e+01±7.77e-02 (+) | 6.32e+01±9.28e-02 (+) | 6.25e+01±1.99e-02 (≈) |
| F4 | D1 | **9.93e-02±3.70e-02** | 4.89e+01±2.23e-01 (+) | 4.43e+00±1.17e+00 (+) | 6.28e+00±4.49e-01 (+) | 6.39e+01±1.06e+00 (+) | 1.60e+02±7.63e-01 (+) | 1.12e+02±1.82e+01 (+) | 2.72e-01±1.67e-02 (+) |
| | D2 | **2.25e+00±2.02e-01** | 5.79e+01±1.01e+00 (+) | 2.58e+01±3.22e-01 (+) | 6.54e+01±1.41e+01 (+) | 4.35e+01±1.10e+00 (+) | 1.36e+02±9.00e-01 (+) | 9.46e+01±6.39e+00 (+) | 2.39e+01±1.62e-01 (+) |
| | D3 | **9.56e+00±3.49e-02** | 5.87e+01±2.14e-01 (+) | 2.65e+01±3.02e-01 (+) | 6.97e+01±6.17e+01 (+) | 4.90e+01±3.62e+00 (+) | 1.12e+02±1.92e+00 (+) | 7.22e+01±5.19e+00 (+) | 1.08e+01±4.00e-01 (+) |
| | D4 | **1.35e+01±1.48e-01** | 6.81e+01±9.64e-01 (+) | 4.94e+01±4.21e-01 (+) | 1.15e+02±6.34e+01 (+) | 6.00e+01±2.38e+00 (+) | 1.04e+02±6.73e-01 (+) | 6.38e+01±6.42e+00 (+) | 1.55e+01±2.89e-01 (≈) |
| | D5 | **9.43e+00±3.49e-01** | 7.16e+01±5.56e-01 (+) | 4.74e+01±3.66e-01 (+) | 1.14e+02±3.90e+01 (+) | 6.26e+01±3.42e+00 (+) | 1.10e+02±1.61e+00 (+) | 7.43e+01±1.60e+01 (+) | 2.00e+01±5.00e-01 (+) |
| F5 | D1 | **4.86e+01±1.70e+00** | 2.00e+03±2.27e+01 (+) | 1.37e+02±6.09e-01 (+) | 1.18e+02±1.46e+01 (+) | 2.63e+03±1.10e+02 (+) | 3.09e+03±3.20e+01 (+) | 3.87e+03±5.64e+02 (+) | 5.18e+01±3.57e+00 (+) |
| | D2 | **3.31e+02±3.14e+00** | 3.37e+03±5.50e+01 (+) | 8.94e+02±1.52e+01 (+) | 9.73e+02±1.63e+02 (+) | 2.02e+03±9.67e+01 (+) | 3.57e+03±6.25e+01 (+) | 4.93e+03±5.50e+02 (+) | 3.86e+02±3.78e+01 (≈) |
| | D3 | **3.88e+02±3.80e+01** | 2.80e+03±3.48e+01 (+) | 8.55e+02±3.29e+00 (+) | 6.35e+03±3.02e+02 (+) | 2.82e+03±1.57e+02 (+) | 4.32e+03±3.94e+01 (+) | 2.52e+03±2.24e+02 (+) | 4.28e+02±9.18e+01 (+) |
| | D4 | **6.12e+02±4.99e+01** | 3.73e+03±3.31e+01 (+) | 2.19e+03±8.32e+00 (+) | 7.22e+03±4.96e+03 (+) | 3.13e+03±9.25e+01 (+) | 4.49e+03±4.33e+01 (+) | 3.53e+03±1.72e+03 (+) | 7.91e+02±3.54e+01 (+) |
| | D5 | **9.30e+02±5.49e+02** | 3.93e+03±2.52e+01 (+) | 2.19e+03±8.51e+01 (+) | 3.13e+03±1.65e+03 (+) | 3.31e+03±1.68e+02 (+) | 4.56e+03±4.92e+01 (+) | 3.17e+03±4.10e+02 (+) | 1.00e+03±1.71e+02 (≈) |
| F6 | D1 | **7.25e+00±1.03e+00** | 2.03e+01±1.19e-02 (+) | 1.28e+01±9.44e-02 (+) | 1.31e+02±1.61e+02 (+) | 2.06e+01±3.54e-02 (+) | 2.09e+01±6.94e-01 (+) | 2.11e+01±3.58e-02 (+) | 8.18e+00±1.04e+00 (+) |
| | D2 | **9.66e+00±2.95e-01** | 2.09e+01±1.54e-02 (+) | 1.80e+01±3.42e-02 (+) | 3.70e+01±7.40e+00 (+) | 2.02e+01±3.84e-02 (+) | 2.10e+01±8.47e-01 (+) | 2.12e+01±6.25e-02 (+) | 1.30e+01±9.21e-01 (+) |
| | D3 | **1.10e+01±9.43e-01** | 2.07e+01±3.88e-02 (+) | 1.93e+01±2.95e-02 (+) | 2.16e+01±9.05e+00 (+) | 2.01e+01±5.75e-02 (+) | 2.11e+01±1.42e-01 (+) | 2.12e+01±3.67e-02 (+) | 1.73e+01±1.66e-01 (+) |
| | D4 | **1.34e+00±2.51e-01** | 2.09e+01±1.28e+00 (+) | 1.93e+01±1.10e-02 (+) | 3.50e+01±9.60e+00 (+) | 2.06e+01±3.92e-02 (+) | 2.12e+01±4.36e-01 (+) | 2.13e+01±1.79e-02 (+) | 1.74e+01±2.82e-01 (≈) |
| | D5 | **1.37e+01±2.51e-01** | 2.09e+01±1.23e+00 (+) | 1.92e+01±1.64e-02 (+) | 2.74e+01±8.88e+00 (+) | 2.07e+01±3.79e-02 (+) | 2.12e+01±1.37e+00 (+) | 2.13e+01±2.12e-02 (+) | 1.70e+01±5.42e-01 (+) |
| F7 | D1 | **4.75e-01±1.46e-01** | 1.01e+00±2.84e+00 (+) | 5.83e-01±5.18e-01 (+) | 3.35e+01±1.99e+01 (+) | 1.00e+00±5.44e+00 (+) | 1.02e+00±3.11e+00 (+) | 1.03e+00±7.85e-01 (+) | 5.09e-01±1.19e-01 (+) |
| | D2 | **6.53e-01±1.13e-01** | 1.02e+00±1.68e+00 (+) | 9.04e-01±3.49e+00 (+) | 9.31e-01±9.42e-02 (+) | 1.01e+00±1.09e-01 (+) | 1.02e+00±2.30e-02 (+) | 1.03e+00±7.74e-01 (+) | 7.30e-01±1.49e-01 (≈) |
| | D3 | **8.13e-01±1.38e-02** | 1.02e+00±4.21e-01 (+) | 1.00e+00±2.77e+00 (+) | 1.71e+00±2.83e-01 (+) | 1.02e+00±6.90e-01 (+) | 1.02e+00±1.26e+00 (+) | 1.02e+00±2.24e+00 (+) | 1.01e+00±2.71e-02 (+) |
| | D4 | **8.77e-01±1.16e-02** | 1.02e+00±5.78e-01 (+) | 9.50e-01±8.15e-01 (+) | 2.31e+00±6.68e-01 (+) | 1.02e+00±4.38e-02 (+) | 1.03e+00±5.77e-01 (+) | 1.03e+00±5.95e-01 (+) | 9.34e-01±4.53e-02 (+) |
| | D5 | **6.71e-01±1.01e-02** | 1.02e+00±1.90e+00 (+) | 9.50e-01±7.68e-01 (+) | 1.89e+00±5.37e-01 (+) | 1.02e+00±1.54e-01 (+) | 1.03e+00±1.60e+00 (+) | 1.02e+00±2.62e-01 (+) | 9.79e-01±1.09e-02 (+) |
| F8 | D1 | **9.40e+01±2.94e+00** | 1.56e+02±3.21e-01 (+) | 1.07e+02±6.11e-01 (+) | 1.04e+02±1.40e+00 (+) | 1.67e+02±9.15e-01 (+) | 1.63e+02±5.80e-01 (+) | 2.33e+02±5.20e+00 (+) | 1.07e+02±4.16e+00 (+) |
| | D2 | **1.01e+02±2.09e+00** | 1.68e+02±1.10e+00 (+) | 1.32e+02±8.29e-01 (+) | 1.84e+02±5.19e+01 (+) | 1.51e+02±1.22e+00 (+) | 1.69e+02±2.94e-01 (+) | 2.10e+02±2.19e+00 (+) | 1.18e+02±2.32e+00 (+) |
| | D3 | **7.71e+01±1.91e+00** | 1.64e+02±4.25e-01 (+) | 1.35e+02±5.32e-01 (+) | 6.35e+02±4.39e-01 (+) | 1.57e+02±2.14e+00 (+) | 1.68e+02±3.39e-01 (+) | 1.87e+02±4.64e+00 (+) | 1.22e+02±1.89e+00 (+) |
| | D4 | **9.58e+01±1.62e+00** | 1.74e+02±3.42e-01 (+) | 1.51e+02±3.55e-01 (+) | 2.52e+02±9.68e+01 (+) | 1.66e+02±1.25e+00 (+) | 1.78e+02±3.11e+00 (+) | 1.77e+02±6.45e+00 (+) | 1.07e+02±1.40e+00 (≈) |
| | D5 | **1.16e+02±7.36e+00** | 1.75e+02±5.29e-01 (+) | 1.51e+02±7.73e-02 (+) | 2.01e+02±7.23e+01 (+) | 1.67e+02±1.55e+00 (+) | 1.76e+02±1.59e+00 (+) | 1.92e+02±3.54e+00 (+) | 1.26e+02±2.00e+00 (≈) |

Table 5: Comparison of the mean and standard deviation over 11 independent runs of $E_{\mathrm{DT}}$ values achieved by different SDDEAs on the DBG benchmark with 10-dimensional decision variables.

| Instance | Drift | TRACE-EA | SAEF-1GP | BDDEA-LDG | TT-DDEA | DSEMFS | DETO | MLDE | DASE |
|---|---|---|---|---|---|---|---|---|---|
| F1 | D1 | **5.22e+01±1.68e+00** | 6.25e+01±1.96e+00 (+) | 6.18e+01±3.32e-02 (+) | 5.91e+01±1.78e+00 (+) | 5.26e+01±6.31e-02 (+) | 6.02e+01±2.98e+00 (+) | 6.20e+01±1.13e+00 (+) | 5.92e+01±2.02e+00 (+) |
| | D2 | **3.90e+01±6.37e-01** | 6.32e+01±2.49e-02 (+) | 6.22e+01±9.61e-02 (+) | 5.92e+01±2.15e-02 (+) | 6.32e+01±8.40e-02 (+) | 6.16e+01±3.74e-01 (+) | 5.94e+01±9.66e-01 (+) | 5.91e+01±1.27e+00 (+) |
| | D3 | **4.37e+01±1.78e-01** | 5.35e+01±8.26e-01 (+) | 5.78e+01±7.10e-02 (+) | 6.01e+01±3.28e-01 (+) | 5.36e+01±1.12e-01 (+) | 5.99e+01±8.62e-01 (+) | 5.72e+01±3.24e+00 (+) | 5.69e+01±2.04e+00 (+) |
| | D4 | **2.59e+01±9.10e-01** | 1.93e+03±9.50e-01 (+) | 1.91e+03±1.14e-01 (+) | 5.31e+01±2.25e+00 (+) | 1.91e+03±7.93e+00 (+) | 5.43e+01±4.05e-01 (+) | 5.43e+01±5.63e+00 (+) | 5.23e+01±1.08e-01 (+) |
| | D5 | **4.23e+01±3.19e+00** | 5.19e+01±4.22e-02 (+) | 4.83e+01±4.85e-02 (+) | 5.22e+01±9.48e-01 (+) | 4.98e+01±2.03e+00 (+) | 5.65e+01±2.44e+00 (+) | 4.56e+01±3.88e-02 (+) | 4.90e+01±2.99e-01 (+) |
| | D6 | **3.74e+01±1.36e-01** | 5.39e+01±3.89e-02 (+) | 5.13e+01±1.52e-02 (+) | 5.30e+01±1.37e+00 (+) | 5.25e+01±1.10e-01 (+) | 5.66e+01±5.67e-02 (+) | 4.72e+01±9.70e-01 (+) | 5.03e+01±6.05e-01 (+) |
| F2 | D1 | **6.31e+01±1.81e-01** | 7.83e+02±3.43e+00 (+) | 8.92e+02±6.58e-01 (+) | 8.37e+01±3.35e-01 (+) | 8.69e+02±3.78e+00 (+) | 9.81e+01±1.33e+00 (+) | 1.19e+02±3.01e+00 (+) | 8.13e+01±1.01e+00 (+) |
| | D2 | **6.75e+01±1.05e+00** | 7.92e+02±3.13e+00 (+) | 5.03e+02±4.14e-01 (+) | 8.49e+01±1.39e+00 (+) | 8.72e+02±6.98e+00 (+) | 9.96e+01±3.92e-01 (+) | 1.19e+02±1.17e+00 (+) | 8.38e+01±1.65e+00 (+) |
| | D3 | **6.99e+01±3.09e+00** | 7.85e+02±2.30e+00 (+) | 4.93e+02±6.12e-01 (+) | 8.33e+01±1.27e-02 (+) | 8.60e+02±3.30e+00 (+) | 9.77e+01±2.62e+00 (+) | 1.14e+02±1.31e+00 (+) | 8.30e+01±3.11e-01 (+) |
| | D4 | **6.07e+01±1.36e-01** | 1.30e+03±4.63e+00 (+) | 1.10e+03±1.21e+00 (+) | 7.42e+01±1.58e+00 (+) | 1.18e+03±6.07e+01 (+) | 8.86e+01±1.01e+00 (+) | 9.44e+01±7.35e-01 (+) | 6.95e+01±4.43e-01 (+) |
| | D5 | **3.46e+01±1.79e+00** | 7.24e+02±3.73e+00 (+) | 4.61e+02±1.16e-01 (+) | 8.44e+01±6.82e-01 (+) | 7.32e+02±3.11e+01 (+) | 9.77e+01±2.52e+00 (+) | 1.14e+02±2.81e+00 (+) | 8.25e+01±7.81e-01 (+) |
| | D6 | **5.94e+01±8.47e-01** | 7.28e+02±3.45e+00 (+) | 4.61e+02±4.56e-01 (+) | 8.43e+01±4.16e+00 (+) | 7.26e+02±1.16e+01 (+) | 8.86e+01±1.55e+00 (+) | 1.15e+02±2.50e+00 (+) | 8.27e+01±8.42e-01 (+) |
| F3 | D1 | **6.72e+01±5.14e-01** | 1.26e+03±2.30e+00 (+) | 1.03e+03±6.40e-01 (+) | 1.01e+02±1.05e+00 (+) | 1.32e+03±7.22e+00 (+) | 1.15e+02±9.02e-01 (+) | 1.28e+02±3.89e+00 (+) | 1.01e+02±2.56e+00 (+) |
| | D2 | **9.40e+01±2.31e+00** | 1.28e+03±1.79e+00 (+) | 1.04e+03±4.30e-01 (+) | 1.02e+02±4.69e+00 (+) | 1.33e+03±6.55e+00 (+) | 1.17e+02±1.08e+00 (+) | 1.31e+02±7.06e-01 (+) | 1.01e+02±3.81e+00 (+) |
| | D3 | **6.86e+01±6.19e-01** | 1.27e+03±2.73e+00 (+) | 1.03e+03±6.55e-01 (+) | 1.02e+02±1.74e+00 (+) | 1.33e+03±4.51e+00 (+) | 1.14e+02±2.08e+00 (+) | 1.30e+02±3.24e+00 (+) | 1.01e+02±2.83e+00 (+) |
| | D4 | **6.45e+01±3.36e+00** | 1.80e+03±7.05e+00 (+) | 1.62e+03±9.93e-01 (+) | 9.16e+01±1.60e+00 (+) | 1.69e+03±3.47e+01 (+) | 1.04e+02±5.78e-01 (+) | 1.16e+02±3.06e+00 (+) | 8.87e+01±1.66e+00 (+) |
| | D5 | **9.56e+01±3.36e-01** | 1.22e+03±2.63e+00 (+) | 1.01e+03±1.99e-01 (+) | 1.02e+02±2.34e+00 (+) | 1.21e+03±2.19e+01 (+) | 1.16e+02±3.82e-01 (+) | 1.28e+02±1.13e+00 (+) | 1.01e+02±6.62e-01 (+) |
| | D6 | **7.37e+01±3.01e+00** | 1.23e+03±5.45e+00 (+) | 1.01e+03±1.49e-01 (+) | 1.02e+02±1.77e+00 (+) | 1.20e+03±6.03e+00 (+) | 1.16e+02±4.02e-01 (+) | 1.29e+02±3.97e+00 (+) | 1.01e+02±2.64e+00 (+) |
| F4 | D1 | **7.00e+01±3.83e-01** | 8.28e+02±4.91e+00 (+) | 4.93e+02±2.92e-01 (+) | 8.44e+01±3.17e+00 (+) | 8.47e+02±8.23e+00 (+) | 1.01e+02±1.15e+00 (+) | 1.18e+02±1.49e+00 (+) | 8.38e+01±2.35e+00 (+) |
| | D2 | **8.04e+01±5.23e+00** | 8.41e+02±2.95e+00 (≈) | 4.93e+02±8.13e-01 (+) | 8.64e+01±1.04e+00 (+) | 8.54e+02±3.92e+00 (+) | 1.03e+02±1.21e+00 (+) | 1.19e+02±1.86e+00 (+) | 8.48e+01±1.87e+00 (+) |
| | D3 | **3.83e+01±1.40e+00** | 8.31e+02±2.02e+00 (+) | 4.94e+02±4.64e-02 (+) | 8.55e+01±6.06e-01 (+) | 8.50e+02±4.03e+00 (+) | 1.00e+02±2.62e+00 (+) | 1.15e+02±2.08e+00 (+) | 8.31e+01±1.47e+00 (+) |
| | D4 | **4.21e+01±2.45e+00** | 1.35e+03±5.71e+00 (+) | 8.58e+02±1.39e+00 (+) | 7.61e+01±1.62e+00 (+) | 7.85e+02±4.27e+01 (+) | 8.70e+01±1.28e+00 (+) | 1.01e+02±1.16e+00 (+) | 7.13e+01±2.25e+00 (+) |
| | D5 | **7.93e+01±2.05e+00** | 7.75e+02±5.15e+00 (+) | 4.52e+02±6.35e-01 (+) | 8.64e+01±2.06e+00 (+) | 7.08e+02±2.50e+01 (+) | 1.01e+02±9.88e-01 (+) | 1.13e+02±1.09e+00 (+) | 8.40e+01±5.41e-01 (+) |
| | D6 | **5.88e+01±8.35e-01** | 7.78e+02±5.41e+00 (+) | 4.52e+02±1.67e-01 (+) | 8.62e+01±9.64e-01 (+) | 6.97e+02±4.69e+00 (+) | 1.01e+02±2.77e+00 (+) | 1.17e+02±9.20e-01 (+) | 8.40e+01±2.52e+00 (+) |
| F5 | D1 | **8.18e+01±2.12e-01** | 1.97e+03±4.67e-01 (+) | 1.87e+03±3.98e-01 (+) | 1.32e+02±2.17e-02 (+) | 1.92e+03±7.75e-01 (+) | 1.28e+02±2.84e+00 (+) | 1.30e+02±3.11e-01 (+) | 1.33e+02±1.63e+00 (+) |
| | D2 | **1.26e+02±4.96e+00** | 1.98e+03±2.70e-01 (+) | 1.87e+03±2.51e-01 (+) | 1.34e+02±1.71e+00 (≈) | 1.92e+03±4.48e-01 (+) | 1.30e+02±7.58e-02 (≈) | 1.33e+02±2.84e+00 (≈) | 1.34e+02±4.23e-01 (+) |
| | D3 | **7.00e+01±2.68e-01** | 1.97e+03±2.92e-01 (+) | 1.87e+03±5.83e-01 (+) | 1.33e+02±4.47e+00 (+) | 1.92e+03±7.25e-01 (+) | 1.27e+02±1.30e+00 (+) | 1.32e+02±4.42e+00 (+) | 1.33e+02±3.53e+00 (+) |
| | D4 | **1.20e+02±4.43e+00** | 2.53e+03±6.10e+00 (+) | 4.94e+02±1.93e+00 (+) | 1.22e+02±2.67e+00 (≈) | 4.86e+02±3.45e+01 (+) | 1.18e+02±4.45e+00 (≈) | 1.19e+02±1.27e-01 (-) | 1.35e+02±1.30e+00 (+) |
| | D5 | **1.12e+02±4.07e+00** | 1.97e+03±8.96e-01 (+) | 1.85e+03±3.80e-01 (+) | 1.34e+02±3.53e+00 (≈) | 1.90e+03±1.37e+01 (+) | 1.29e+02±5.34e+00 (+) | 1.32e+02±1.41e+00 (+) | 1.35e+02±2.00e+00 (+) |
| | D6 | **1.25e+02±4.88e-02** | 1.97e+03±4.64e-01 (+) | 1.85e+03±7.38e-01 (+) | 1.34e+02±2.36e+00 (≈) | 1.90e+03±7.57e+00 (+) | 1.29e+02±4.47e+00 (≈) | 1.33e+02±8.09e-02 (≈) | 1.35e+02±1.36e+00 (+) |
| F6 | D1 | **1.05e+02±1.06e+00** | 1.45e+03±1.76e+00 (+) | 1.18e+03±2.66e-01 (≈) | 1.06e+02±8.85e-01 (≈) | 1.43e+03±3.60e+00 (+) | 1.19e+02±9.78e-01 (+) | 1.28e+02±6.85e-01 (+) | 1.34e+02±7.30e-01 (+) |
| | D2 | **1.04e+02±9.11e-02** | 1.46e+03±1.53e+00 (+) | 1.18e+03±9.67e-01 (+) | 1.07e+02±1.20e+00 (≈) | 1.44e+03±3.28e+00 (+) | 1.20e+02±5.18e+00 (+) | 1.31e+02±2.27e-01 (+) | 1.36e+02±1.41e+00 (+) |
| | D3 | **1.19e+02±5.78e-01** | 1.45e+03±1.53e+00 (+) | 1.18e+03±5.21e-01 (+) | 1.06e+02±1.56e+00 (-) | 1.43e+03±4.48e+00 (+) | 1.20e+02±3.33e-01 (≈) | 1.29e+02±1.16e+00 (+) | 1.33e+02±1.12e-02 (+) |
| | D4 | **1.13e+02±2.57e-01** | 1.95e+03±8.50e+00 (+) | 2.17e+02±1.03e+00 (+) | 9.58e+01±8.80e-01 (-) | 2.04e+02±2.37e+01 (+) | 1.20e+02±1.56e+00 (+) | 1.19e+02±2.00e+00 (≈) | 1.46e+02±5.43e+00 (+) |
| | D5 | **1.05e+02±5.68e-02** | 1.39e+03±2.28e+00 (+) | 1.13e+03±4.15e-01 (+) | 1.07e+02±4.48e-01 (≈) | 1.31e+03±3.01e+01 (+) | 1.20e+02±2.47e+00 (+) | 1.30e+02±5.80e+00 (+) | 1.35e+02±4.68e-01 (+) |
| | D6 | **9.45e+01±1.99e-01** | 1.39e+03±2.20e+00 (+) | 1.12e+03±1.09e+00 (+) | 1.06e+02±5.14e-01 (+) | 1.28e+03±6.99e-01 (+) | 1.20e+02±6.41e-01 (+) | 1.31e+02±2.68e+00 (+) | 1.35e+02±3.02e-01 (+) |

Table 6: Comparison of the mean and standard deviation over 11 independent runs of $E_{\mathrm{DT}}$ values achieved by different SDDEAs on the GMPB benchmark with 10-dimensional decision variables.

| Instance | TRACE-EA | SAEF-1GP | BDDEA-LDG | TT-DDEA | DSEMFS | DETO | MLDE | DASE |
|---|---|---|---|---|---|---|---|---|
| F1 | **8.15e+02±1.12e+01** | 1.45e+03±1.44e+01 (+) | 1.04e+03±2.46e+00 (+) | 1.19e+03±4.53e+01 (+) | 1.10e+02±1.02e+01 (+) | 1.13e+03±1.10e+01 (+) | 1.17e+03±4.52e+01 (+) | 1.31e+03±4.10e+01 (+) |
| F2 | **5.35e+02±6.67e+00** | 6.73e+02±1.19e+01 (+) | 7.59e+02±1.37e+01 (+) | 7.64e+02±1.98e+01 (+) | 7.37e+02±3.83e+01 (+) | 7.16e+02±4.89e+00 (+) | 7.70e+02±5.08e+01 (+) | 8.29e+02±2.47e+01 (+) |
| F3 | **1.01e+03±1.36e+01** | 1.58e+03±1.51e+01 (+) | 1.42e+03±1.38e+01 (+) | 1.31e+03±5.63e+01 (+) | 1.17e+03±1.85e+01 (+) | 1.31e+03±1.13e+01 (+) | 1.47e+03±6.54e+01 (+) | 1.40e+03±5.71e+01 (+) |
| F4 | **4.95e+02±5.29e+00** | 5.64e+02±1.20e+01 (≈) | 6.13e+02±4.02e+01 (+) | 8.58e+02±6.61e+01 (+) | 5.10e+02±1.45e+01 (+) | 7.27e+02±9.26e+00 (+) | 9.04e+02±5.57e+01 (+) | 9.29e+02±3.52e+01 (+) |
| F5 | **8.58e+02±7.89e+00** | 9.89e+03±4.77e+01 (+) | 1.66e+03±2.71e+01 (+) | 1.03e+03±3.31e+02 (+) | 1.73e+03±4.13e+01 (+) | 1.07e+03±4.18e+00 (+) | 1.05e+03±2.65e+02 (+) | 1.14e+03±4.08e+02 (+) |
| F6 | **4.20e+02±3.97e+00** | 4.57e+02±6.50e+01 (≈) | 9.31e+02±4.31e+01 (+) | 8.27e+02±1.23e+02 (+) | 5.53e+02±5.96e+01 (+) | 9.89e+02±9.62e+00 (+) | 8.85e+02±9.97e+01 (+) | 8.94e+02±7.75e+01 (+) |
| F7 | **1.01e+03±9.75e+00** | 1.78e+03±4.37e+01 (+) | 1.46e+03±4.53e+01 (+) | 1.40e+03±3.32e+02 (+) | 1.64e+03±2.72e+01 (+) | 1.47e+03±1.87e+01 (+) | 1.25e+03±4.31e+02 (+) | 1.49e+03±3.17e+02 (+) |
| F8 | **8.64e+02±7.43e+00** | 1.50e+03±6.30e+01 (+) | 2.50e+03±1.01e+02 (+) | 1.12e+03±2.58e+02 (+) | 2.19e+03±7.72e+01 (+) | 1.04e+03±1.38e+01 (+) | 1.12e+03±1.59e+02 (+) | 9.68e+02±2.57e+02 (+) |

Table 7: The performance results of the TRACE's plug-and-play capability on SDDObench.

| Instance | Drift | TRACE-EA | DASE | DETO+TRACE | DETO | TT-DDEA+TRACE | TT-DDEA | MLDE+TRACE | MLDE |
|---|---|---|---|---|---|---|---|---|---|
| F1 | D1 | **6.52e+01±1.52e-02** | 6.55e+01±2.23e-02 | 6.75e+01±3.65e+00 (≈) | 6.81e+01±8.02e+00 | 6.70e+01±1.12e+00 (↑) | 6.80e+01±1.61e+00 | 6.67e+01±5.40e-02 (≈) | 6.81e+01±3.65e-02 |
| | D2 | **6.53e+01±4.90e-01** | 6.61e+01±1.33e-01 | 6.62e+01±1.06e+00 (↑) | 6.70e+01±2.42e+00 | 6.60e+01±1.92e+00 (↑) | 6.68e+01±1.08e+00 | 6.68e+01±2.40e-02 (≈) | 6.70e+01±3.33e-02 |
| | D3 | **6.37e+01±1.42e-01** | 6.40e+01±2.51e-01 | 6.55e+01±5.84e+00 (≈) | 6.59e+01±3.03e-01 | 6.50e+01±9.00e-01 (↑) | 6.57e+01±3.11e+00 | 6.52e+01±9.14e-02 (≈) | 6.59e+01±1.95e-02 |
| | D4 | **6.40e+01±1.77e-01** | 6.39e+01±1.33e-01 | 6.49e+01±4.94e-01 (≈) | 6.51e+01±4.40e-01 | 6.40e+01±2.35e+00 (≈) | 6.49e+01±1.86e+00 | 6.48e+01±1.87e-02 (≈) | 6.51e+01±5.06e-02 |
| | D5 | **6.41e+01±1.73e-01** | 6.45e+01±1.04e-01 | 6.46e+01±3.67e-02 (≈) | 6.53e+01±7.73e-02 | 6.48e+01±5.47e-02 (≈) | 6.51e+01±2.28e-02 | 6.48e+01±7.30e-02 (≈) | 6.52e+01±3.92e-02 |
| F2 | D1 | **6.69e+01±6.51e-01** | 6.76e+01±2.64e-01 | 6.77e+01±2.00e+00 (≈) | 6.81e+01±2.47e+00 | 6.77e+01±1.70e+00 (≈) | 6.80e+01±4.53e+00 | 6.75e+01±3.94e-02 (≈) | 6.81e+01±7.82e-02 |
| | D2 | **6.52e+01±4.50e-01** | 6.68e+01±1.56e-01 | 6.66e+01±5.06e-01 (↑) | 6.73e+01±4.86e-01 | 6.72e+01±1.22e-01 (≈) | 6.74e+01±5.60e-01 | 6.68e+01±1.16e-01 (≈) | 6.72e+01±5.40e-01 |
| | D3 | **6.50e+01±3.33e-01** | 6.54e+01±4.10e-01 | 6.69e+01±1.93e+00 (≈) | 6.72e+01±1.62e+00 | 6.68e+01±3.40e-01 (≈) | 6.70e+01±6.14e-01 | 6.71e+01±1.34e-01 (≈) | 6.75e+01±4.17e-01 |
| | D4 | **6.40e+01±6.93e-01** | 6.43e+01±7.32e-01 | 6.60e+01±2.49e+00 (↑) | 6.67e+01±3.05e+00 | 6.68e+01±2.36e-01 (≈) | 6.72e+01±1.06e-01 | 6.69e+01±1.58e-01 (≈) | 6.70e+01±8.26e-01 |
| | D5 | **6.44e+01±7.12e-01** | 6.52e+01±1.02e-02 | 6.60e+01±4.75e-01 (≈) | 6.64e+01±3.41e-01 | 6.73e+01±1.53e-01 (≈) | 6.75e+01±9.29e-01 | 6.70e+01±3.00e-01 (≈) | 6.73e+01±9.46e-01 |
| F3 | D1 | **6.70e+01±1.03e-01** | 6.77e+01±1.26e-02 | 6.77e+01±1.03e-01 (↑) | 6.81e+01±6.29e-01 | 6.77e+01±7.22e-01 (≈) | 6.80e+01±5.76e-01 | 6.69e+01±9.15e-02 (≈) | 6.81e+01±1.90e-02 |
| | D2 | **6.50e+01±1.14e-01** | 6.58e+01±7.68e-02 | 6.60e+01±2.38e-02 (↑) | 6.66e+01±4.83e-02 | 6.59e+01±1.83e-02 (↑) | 6.64e+01±2.72e-02 | 6.45e+01±1.59e-02 (↑) | 6.65e+01±4.12e-02 |
| | D3 | **6.20e+01±2.28e-01** | 6.23e+01±4.11e-02 | 6.29e+01±3.03e+00 (↑) | 6.34e+01±1.05e+00 | 6.29e+01±1.48e-02 (↑) | 6.34e+01±6.65e-02 | 6.26e+01±1.05e-02 (↑) | 6.34e+01±4.80e-02 |
| | D4 | **6.23e+01±1.12e-02** | 6.25e+01±2.08e-02 | 6.29e+01±2.05e+00 (↑) | 6.32e+01±3.01e+00 | 6.25e+01±6.69e-02 (≈) | 6.30e+01±8.35e-02 | 6.29e+01±1.39e-02 (≈) | 6.32e+01±8.46e-02 |
| | D5 | **6.21e+01±1.69e-02** | 6.27e+01±1.99e-02 | 6.30e+01±3.59e-01 (↑) | 6.34e+01±1.90e-01 | 6.28e+01±2.80e-01 (≈) | 6.30e+01±1.44e-01 | 6.26e+01±1.75e-02 (↑) | 6.32e+01±9.28e-02 |
| F4 | D1 | **9.93e-02±3.70e-02** | 2.72e-01±1.67e-02 | 1.35e+02±1.42e+00 (↑) | 1.60e+02±2.22e+00 | 4.96e+00±3.93e+00 (↑) | 6.28e+00±4.49e-01 | 9.81e+01±3.39e+01 (≈) | 1.12e+02±1.82e+01 |
| | D2 | **2.25e+01±2.02e-01** | 2.39e+01±1.62e-01 | 9.95e+01±1.10e+00 (↑) | 1.36e+02±9.00e-01 | 6.26e+01±1.07e+01 (≈) | 6.54e+01±1.41e+01 | 8.51e+01±9.30e+00 (↑) | 9.46e+01±6.39e+00 |
| | D3 | **9.56e+00±3.49e-02** | 1.08e+01±4.00e-01 | 1.04e+02±1.12e+00 (≈) | 1.12e+02±3.87e+00 | 5.64e+01±3.40e+01 (↑) | 6.97e+01±6.17e+01 | 3.92e+01±9.05e-01 (↑) | 7.22e+01±5.19e+00 |
| | D4 | **1.35e+01±1.48e-01** | 1.55e+01±2.89e-01 | 9.29e+01±2.39e+00 (↑) | 1.04e+02±5.39e+00 | 1.03e+02±1.80e+01 (≈) | 1.15e+02±6.34e+01 | 5.13e+01±1.11e+00 (↑) | 6.38e+01±6.42e+00 |
| | D5 | **9.43e+00±3.49e-01** | 2.00e+01±5.00e-01 | 9.09e+01±3.61e+00 (↑) | 1.10e+02±2.36e+00 | 1.02e+02±4.27e+01 (≈) | 1.14e+02±3.90e+01 | 5.76e+01±1.88e+00 (↑) | 7.43e+01±1.60e+01 |
| F5 | D1 | **4.86e+01±1.70e+00** | 5.18e+01±3.57e+00 | 2.85e+03±1.79e+01 (≈) | 3.09e+03±2.85e+01 | 9.50e+01±4.97e+01 (↑) | 1.18e+02±1.46e+01 | 2.62e+03±8.35e+01 (↑) | 3.87e+03±5.64e+02 |
| | D2 | **3.31e+02±3.14e+00** | 3.86e+02±3.78e+01 | 3.16e+03±2.35e+01 (↑) | 3.57e+03±6.25e+01 | 8.50e+02±8.99e+01 (↑) | 9.73e+02±1.63e+02 | 4.68e+03±4.48e+01 (↑) | 4.93e+03±5.50e+01 |
| | D3 | **3.88e+02±3.80e+01** | 4.28e+02±9.18e+01 | 4.07e+03±1.33e+01 (≈) | 4.32e+03±4.02e+01 | 6.09e+02±2.19e+01 (↑) | 6.35e+02±2.03+01 | 9.42e+02±1.16e+01 (↑) | 2.52e+03±2.24e+01 |
| | D4 | **6.12e+02±4.99e+01** | 7.91e+02±3.54e+01 | 4.25e+03±3.08e+01 (↑) | 4.49e+03±4.53e+01 | 6.53e+03±7.70e+02 (↑) | 7.22e+03±4.96e+03 | 1.90e+03±2.13e+02 (↑) | 3.53e+03±1.72e+02 |
| | D5 | **9.30e+02±5.49e+02** | 1.00e+03±1.71e+02 | 4.11e+03±3.23e+01 (↑) | 4.56e+03±4.26e+01 | 2.68e+03±1.40e+03 (≈) | 3.13e+03±1.65e+03 | 2.78e+03±3.13e+02 (↑) | 3.17e+03±4.10e+02 |
| F6 | D1 | **7.25e+00±1.03e+00** | 8.18e+00±1.04e+00 | 1.56e+01±1.33e+00 (↑) | 2.09e+01±1.45e+00 | 9.85e+01±2.88e+02 (≈) | 1.31e+02±1.61e+02 | 1.81e+01±1.86e-02 (↑) | 2.11e+01±3.58e-02 |
| | D2 | **9.66e+00±2.95e-01** | 1.30e+01±9.21e-01 | 1.74e+01±7.74e-01 (≈) | 2.10e+01±3.35e-01 | 3.35e+01±2.53e+00 (≈) | 3.70e+01±7.40e+00 | 1.72e+01±1.85e-02 (↑) | 2.12e+01±6.25e-02 |
| | D3 | **1.10e+01±9.43e-01** | 1.73e+01±1.66e-01 | 1.66e+01±1.59e+00 (↑) | 2.11e+01±1.75e+00 | 1.86e+01±5.27e+00 (≈) | 2.16e+01±9.05e+00 | 1.97e+01±1.51e-02 (≈) | 2.12e+01±3.67e-02 |
| | D4 | **1.34e+01±1.31e-01** | 1.74e+01±2.82e-01 | 1.71e+01±2.18e+00 (≈) | 2.12e+01±2.49e+00 | 3.24e+01±1.48e+00 (↑) | 3.50e+01±9.60e+00 | 1.03e+01±2.77e-02 (↑) | 2.13e+01±1.79e-02 |
| | D5 | **1.37e+01±2.51e-01** | 1.70e+01±5.42e-01 | 1.78e+01±3.15e+00 (↑) | 2.12e+01±1.30e+00 | 2.38e+01±1.02e+00 (↑) | 2.74e+01±8.88e+00 | 1.45e+01±1.51e-02 (≈) | 2.13e+01±2.12e-02 |
| F7 | D1 | **4.75e-01±1.46e-01** | 5.09e-01±1.19e-01 | 8.32e-01±1.09e-01 (↑) | 1.02e+00±2.01e+00 | 2.93e+01±3.39e+00 (↑) | 3.35e+01±1.99e+01 | 9.51e-01±2.96e-01 (↑) | 1.03e+00±1.20e+00 |
| | D2 | **6.53e-01±1.13e-01** | 7.30e-01±1.49e-01 | 9.39e-01±1.41e-01 (↑) | 1.02e+00±5.97e-01 | 7.17e-01±2.20e+00 (↑) | 9.31e-01±9.42e-02 | 8.84e-01±1.86e+00 (↑) | 1.03e+00±2.35e+00 |
| | D3 | **8.13e-01±1.38e-02** | 1.01e+00±2.71e-02 | 9.29e-01±4.90e+00 (↑) | 1.02e+00±1.13e+00 | 1.31e+00±4.20e-01 (≈) | 1.71e+00±2.83e-01 | 7.94e-01±4.65e-01 (↑) | 1.02e+00±1.96e+00 |
| | D4 | **8.77e-01±1.16e-02** | 9.34e-01±4.53e-02 | 9.64e-01±5.14e-01 (↑) | 1.03e+00±7.56e-01 | 1.73e+00±1.83e-01 (↑) | 2.31e+00±6.68e-01 | 8.86e-01±1.39e-01 (↑) | 1.03e+00±2.13e+00 |
| | D5 | **6.71e-01±1.01e-02** | 9.79e-01±1.09e-02 | 8.84e-01±2.12e-01 (↑) | 1.03e+00±6.16e-01 | 9.47e-01±2.20e-01 (↑) | 1.89e+00±5.37e-01 | 7.82e-01±2.33e-01 (↑) | 1.02e+00±3.74e+00 |
| F8 | D1 | **9.40e+01±2.94e+00** | 1.07e+02±4.16e+00 | 1.39e+02±2.93e+00 (≈) | 1.63e+02±2.93e+00 | 9.47e+01±1.51e+00 (↑) | 1.24e+02±1.40e+00 | 1.73e+02±1.47e+00 (↑) | 2.33e+02±5.20e+00 |
| | D2 | **1.01e+02±2.09e+00** | 1.18e+02±2.32e+00 | 1.42e+02±2.62e-01 (↑) | 1.69e+02±2.94e-01 | 2.43e+02±1.79e+00 (≈) | 2.84e+02±5.19e+00 | 1.88e+02±8.04e-01 (↑) | 2.10e+02±2.19e+00 |
| | D3 | **7.71e+01±1.91e+00** | 1.22e+02±1.89e+00 | 1.48e+02±1.87e+00 (≈) | 1.68e+02±1.44e+00 | 2.05e+02±2.65e+00 (↑) | 2.35e+02±1.32e+00 | 1.13e+02±1.40e+00 (↑) | 1.87e+02±4.64e+00 |
| | D4 | **9.58e+01±1.62e+00** | 1.07e+02±1.40e+00 | 1.50e+02±1.15e+00 (↑) | 1.78e+02±3.63e+00 | 2.06e+02±1.43e+01 (↑) | 2.52e+02±9.68e+01 | 9.45e+01±2.90e+00 (↑) | 1.77e+02±6.45e+00 |
| | D5 | **1.16e+02±7.36e+00** | 1.26e+02±2.00e+00 | 1.45e+02±7.17e+00 (↑) | 1.76e+02±1.89e+00 | 1.82e+02±1.52e+01 (≈) | 2.01e+02±7.23e+01 | 1.33e+02±3.20e+00 (↑) | 1.92e+02±3.54e+00 |

Table 8: The Average Detection Delay Time on SDDObench_F4

| Drift types | Intensity | TRACE | DDM | ADWIN | HDDM_A | HDDM_W | FHDDM | KSWIN | RADAR | MCD-DD | HCDD |
|---|---|---|---|---|---|---|---|---|---|---|---|
| Sudden drift (D2) | $\mathcal{I}_x = 0.2$ | 96.0 | 235.1 | 190.1 | 210.2 | 215.5 | 170.7 | 195.5 | 123.2 | 116.7 | **94.3** |
| | $\mathcal{I}_x = 0.4$ | 88.0 | 210.2 | 188.6 | 223.3 | 234.2 | 176.6 | 190.1 | 122.1 | 114.9 | **85.2** |
| | $\mathcal{I}_x = 0.6$ | **82.0** | 188.4 | 150.2 | 200.1 | 181.9 | 166.5 | 185.4 | 115.5 | 110.3 | 83.1 |
| Recurrent incremental drift (D4) | $P = 10$ | **88.0** | 178.7 | 177.9 | 193.2 | 191.2 | 175.3 | 198.0 | 129.5 | 113.2 | 88.5 |
| | $P = 20$ | **92.0** | 233.1 | 183.2 | 199.2 | 192.3 | 175.3 | 198.0 | 129.5 | 120.1 | 93.3 |
| | $P = 30$ | **94.0** | 255.9 | 200.1 | 213.9 | 215.2 | 175.3 | 198.0 | 129.5 | 116.2 | 94.3 |

evolving clusters in an online manner without storing the entire data stream. It is particularly relevant in real-time applications such as network intrusion detection, electricity market monitoring, environmental sensing, and user behavior analysis, where data arrives continuously and often exhibits non-stationary distributions.

The details of the four real-world datasets are as follows:

- **Covtype (Blackard and Dean 1999)**: This dataset consists of 581,012 observations with 54 variables, including 10 numeric features, collected from four regions within the Roosevelt National Forest in northern Colorado. The task is to predict forest cover type using only cartographic variables. These cover types are determined by natural ecological processes rather than human activity. The ground truth labels were provided by the U.S. Forest Service, while the input variables were derived from U.S. Geological Survey data.
- **Pokerhand (Asuncion, Newman et al. 2007)**: This dataset contains over 800,000 instances and 10 predictive attributes, of which 5 are numeric. Each instance represents a poker hand consisting of five cards drawn from a standard 52-card deck. Each card is described by two attributes, including suit and rank, which can result in a total of 10 attributes. Additionally, the dataset includes one class attribute that specifies the type of poker hand represented.
- **Electricity (Asuncion, Newman et al. 2007)**: This dataset comprises 45,312 observations collected from the Australian New South Wales Electricity Market. In this market, electricity prices fluctuate based on supply and demand. The class label indicates whether the price has increased or decreased relative to a 24-hour moving average. A normalized version of the dataset is used in our experiments.
- **Kddcup99 (KddCup99 2007)**: This dataset contains 4,898,431 records of network traffic data. The former 100,000 records are used in our experiments. Each instance is described by 31 numeric features characterizing the connection, such as protocol type and connection duration. The class label indicates whether the connection is normal or corresponds to one of 22 distinct types of network attacks.

## References

Alsaedi, A.; Sohrabi, N.; Mahmud, R.; and Tari, Z. 2023. RADAR: Reactive concept drift management with robust

Table 9: The Mean Inference Time (MIT) and Peak Memory Usage (PMU) on SDDObench_F4D2

| Metrics | TRACE | DDM | ADWIN | HDDM_A | HDDM_W | FHDDM | KSWIN | RADAR | MCD-DD | HCDD |
|---|---|---|---|---|---|---|---|---|---|---|
| MIT (ms) | 4.2 | 2.6 | 6.2 | 10.1 | 9.8 | 3.4 | 4.1 | 160.1 | 20.1 | 2.3 |
| PMU (CPU, MB) | 119.3 | 19.9 | 120.7 | 212.3 | 221.2 | 34.1 | 53.8 | 2305.7 | 561.3 | 23.8 |
| PMU (GPU, MB) | 385.5 | N/A | N/A | N/A | N/A | N/A | N/A | N/A | N/A | N/A |


variational inference for evolving iot data streams. In *Proceedings of IEEE 39th International Conference on Data Engineering (ICDE)*, 1995–2007.

Asuncion, A.; Newman, D.; et al. 2007. UCI machine learning repository.

Bifet, A.; and Gavaldà, R. 2007. Learning from time-changing data with adaptive windowing. In *Proceedings of the 2007 SIAM International Conference on Data Mining*, 443–448.

Blackard, J. A.; and Dean, D. J. 1999. Comparative accuracies of artificial neural networks and discriminant analysis in predicting forest cover types from cartographic variables. *Computers and Electronics in Agriculture*, 24(3): 131–151.

Chen, L.; and Shang, S. 2019. Region-based message exploration over spatio-temporal data streams. In *Proceedings of the AAAI conference on artificial intelligence*, volume 33, 873–880.

Frias-Blanco, I.; Campo-Avila, J. D.; Ramos-Jimenez, G.; Morales-Bueno, R.; Ortiz-Diaz, A.; and Caballero-Mota, Y. 2015. Online and Non-Parametric Drift Detection Methods Based on Hoeffding's Bounds. *IEEE Transactions on Knowledge and Data Engineering*, 27(3): 810–823.

Gama, J.; Medas, P.; Castillo, G.; and Rodrigues, P. 2004. Learning with drift detection. In *Proceeding of Advances in Artificial Intelligence–SBIA 2004: 17th Brazilian Symposium on Artificial Intelligence*, 286–295.

Huang, P.; Wang, H.; and Jin, Y. 2021. Offline data-driven evolutionary optimization based on tri-training. *Swarm and Evolutionary Computation*, 60: 100800.

KddCup99. 2007. https://kdd.ics.uci.edu/databases/kddcup99/kddcup99.html.

Li, C.; Yang, S.; Nguyen, T.-T.; Yu, E. L.; Yao, X.; Jin, Y.; Beyer, H.; and Suganthan, P. N. 2008. Benchmark generator for CEC 2009 competition on dynamic optimization. Technical report.

Li, J.-Y.; Zhan, Z.-H.; Wang, C.; Jin, H.; and Zhang, J. 2020. Boosting data-driven evolutionary algorithm with localized data generation. *IEEE Transactions on Evolutionary Computation*, 24(5): 923–937.

Li, K.; Chen, R.; and Yao, X. 2024. A data-driven evolutionary transfer optimization for expensive problems in dynamic environments. *IEEE Transactions on Evolutionary Computation*, 28(5): 1396–1411.

Luo, W.; Yi, R.; Yang, B.; and Xu, P. 2019. Surrogate-assisted evolutionary framework for data-driven dynamic optimization. *IEEE Transactions on Emerging Topics in Computational Intelligence*, 3(2): 137–150.

Pesaranghader, A.; and Viktor, H. L. 2016. Fast hoeffding drift detection method for evolving data streams. In *Machine Learning and Knowledge Discovery in Databases*, volume 9852, 96–111.

Raab, C.; Heusinger, M.; and Schleif, F.-M. 2020. Reactive soft prototype computing for concept drift streams. *Neurocomputing*, 416: 340–351.

Wan, K.; Liang, Y.; and Yoon, S. 2024. Online drift detection with maximum concept discrepancy. In *Proceedings of the 30th ACM SIGKDD Conference on Knowledge Discovery and Data Mining*, 2924–2935.

Yang, C.; Ding, J.; Jin, Y.; and Chai, T. 2023. A data stream ensemble assisted multifactorial evolutionary algorithm for offline data-driven dynamic optimization. *Evolutionary Computation*, 1–25.

Yazdani, D.; Omidvar, M. N.; Cheng, R.; Branke, J.; Nguyen, T. T.; and Yao, X. 2022. benchmarking continuous dynamic optimization: Survey and generalized test suite. *IEEE Transactions on Cybernetics*, 52(5): 3380–3393.

Zhang, H.; Ding, J.; Feng, L.; Tan, K. C.; and Li, K. 2024. solving expensive optimization problems in dynamic environments with meta-learning. *IEEE Transactions On Cybernetics*.

Zhong, Y.-T.; and Gong, Y.-J. 2025. Data-driven evolutionary computation under continuously streaming environments: A drift-aware approach. *IEEE Transactions on Evolutionary Computation*.

Zhong, Y.-T.; Wang, X.-C.; Sun, Y.-H.; and Gong, Y.-J. 2024. SDDObench: A benchmark for streaming data-driven optimization with concept drift. In *Proceedings of the Genetic and Evolutionary Computation Conference*, 59–67.